G.POT: A quantitative method for the assessment and mapping of the shallow geothermal potential

G.POT: a quantitative method for the assessment and mapping of the shallow geothermal potential

Authors: Alessandro Casasso, Rajandrea Sethi *

* corresponding author

DIATI – Politecnico di Torino, corso Duca degli Abruzzi 24, 10129 Torino (Italy)

Telephone number: +39 0110907735

alessandro.casasso@polito.it , rajandrea.sethi@polito.it

Abstract

Ground source heat pumps (GSHPs) exchange heat with the ground to provide sustainable heating or cooling. Their technological feasibility and economic viability depend on the site-specific thermal properties of the ground and on the usage profile of the plant. These parameters influence the shallow geothermal potential, which is defined as the thermal power that can be efficiently exchanged by a Borehole Heat Exchanger (BHE) of a certain depth. We present a general method (G.POT) for the determination of shallow geothermal potentials. This method was derived using a comprehensive set of analytical heat transfer simulations, performed by varying (i) the thermal properties of the ground, which comprise its thermal conductivity and capacity, (ii) the thermal properties of the borehole, and (iii) the operational and design parameters of the plant, namely, the BHE length, the threshold temperature of the heat carrier fluid, the duration of the heating/cooling season and the simulated lifetime. Therefore, the G.POT method is a simple and flexible tool that can be implemented in a wide range of different scenarios for large-scale mapping of geothermal potentials. We also assess G.POT by discussing its application to map the geothermal yield in the Province of Cuneo (Piemonte, NW Italy).

Keywords

Ground Source Heat Pump; Geothermal potential; Borehole Heat Exchanger; Thermal conductivity; Low enthalpy geothermal energy;

1. Introduction

Ground Source Heat Pumps (GSHPs) have great potential for reducing greenhouse gas emissions in the heating and cooling of buildings [1, 2] and the air pollution in urban environments. Shallow geothermal installations are divided into closed loop plants, in which a heat carrier fluid is circulated through a pipe loop to exchange heat with the surrounding ground, and open loop plants, in which the heat exchange is performed on groundwater [3, 4]. Closed loop plants and, among them, Borehole Heat Exchangers (BHEs), are the most widespread shallow geothermal installations. The use of GSHPs has grown steadily in the last decade [5], although numbers are generally still limited. Diverse limiting factors have hampered the spread of shallow geothermal plants. The cost of drilling the BHEs, which accounts for half of the total expense in small residential installations [6], makes GSHPs significantly more expensive than other technical solutions for the heating and cooling of buildings. GSHPs reduce the cost of the production of heating and cooling and can be considered as a good and safe investment [7]. However, their payback time when replacing a methane boiler is usually in the order of 10 years [8], a value which can be hardly sustainable for industries [9]. Besides the economic factors, the lack of knowledge about the technologies and the advantages of GSHPs is a strong limitation to their growth. To fill this gap, a large number of projects have been carried out in Europe, with demonstration plants, market analyses and the implementation of GSHPs in the energy plans of large cities [10-13]. Another non-technical barrier which limits the spread of shallow geothermal plants is the lack of knowledge on whether the different territories are suitable for such installations. Indeed, the shallow geothermal potential, i.e. the thermal load that can be sustainably exchanged with the ground by a GSHP, depends on the site-specific thermal and hydrogeological properties of the ground. In particular, the efficiency of BHEs mostly depends on the thermal conductivity of the subsurface [14-16], while the thermal advection and dispersion can enhance their performance if a strong groundwater flow is present [17-20]. On the other hand, the operation of GWHPs is affected by the hydraulic properties of the aquifer [21, 22]. A few methods have already been developed for the estimation of the shallow geothermal

potential for closed loop plants, the most common one is the German VDI 4640 norm [23] which provides the value of the extractable power per unit length (W/m) for different lithologies and considering two different usage profiles (1800 and 2400 hours per year). Gemelli et al. [8] adopted this method for assessing the potential of GSHPs in the Marche region (Central Italy), estimating that a BHE length ranging between 80 and 160 m is necessary to satisfy a standard thermal load of 5 kW. The Department of Energy and Climate Change of the United Kingdom provides reference tables to evaluate the geothermal potential of vertical and horizontal closed loop systems, depending on the length of the heating season, the thermal conductivity and the temperature of the ground [24]. These tables can be used for the dimensioning of small closed-loop geothermal plants, however no explicit formula is provided and hence it is difficult to adopt such method for the mapping of the geothermal potential on a large scale. A method was recently developed by Galgaro et al. (2015, [25]) to evaluate the techno-economic feasibility of GSHPs in 4 regions of Southern Italy (Campania, Apulia, Calabria, Sicily), both in heating and cooling mode. This method is based on heat transfer simulations for the calibration of empirical correlations, which are valid on the mapped territory. Garcìa-Gil et al. [26] studied the potential of BHEs and GWHPs in the metropolitan area of Barcelona (Spain), deriving a method for assessing to quantify the maximum thermal power per unit surface that can be exchanged with the ground in such a densely populated urban area.

The aforementioned studies are interesting from different viewpoints, and they have been the basis for a quantitative, flexible and simple approach to evaluate the shallow geothermal potential. We therefore developed a method, called G.POT (Geothermal POTential), to estimate the maximum quantity of heat that can be sustainably exchanged by a Borehole Heat Exchanger during a heating or cooling season. The geothermal potential is an indicator of the economic feasibility for the installation of BHEs at a certain site: the higher the potential, the shorter the BHE(s) to be drilled to provide the required thermal load, and hence the shorter the payback time of the geothermal heat pump compared to other technologies. The conceptual framework and the mathematical model of the G.POT method are presented in the next

paragraph. An example of the application of G.POT for the mapping of geothermal potential in the Province of Cuneo (a 6,900 km^2 wide district in North-Western Italy) is reported and discussed.

2. The G.POT method

The shallow geothermal potential $\bar{Q}_{BHE}$ is the yearly average thermal load that can sustainably be exchanged by a Borehole Heat Exchanger with a length L, for a given ground condition. Sustainable means that $\bar{Q}_{BHE}$ is the highest value of the average thermal load that can be extracted or injected in the ground, without excessive cooling or heating of the heat carrier fluid over the entire life of the system.

The geothermal potential can be calculated both for cooling and for heating mode and it depends on:

- ground thermal properties: thermal conductivity (λ), thermal capacity (ρc) and undisturbed ground temperature (T_0);
- geometrical and thermal properties of BHE: borehole depth (L), borehole radius (r_b) and thermal resistance (R_b);
- minimum (or maximum) temperature of the carrier fluid during heating (or cooling) mode (T_{lim});
- length of heating (or cooling) season (t_c);
- simulation time (t_s): time over which the sustainability of the geo-exchange is evaluated.

The G.POT method provides a general empirical relationship for the calculation of $\bar{Q}_{BHE}$. The assumptions under which $\bar{Q}_{BHE}$ is calculated here are:

- the ground is homogeneous;
- the thermal load of the BHE is annual cyclic with an emi-sinusoidal profile (Fig. 1);
- the BHE is modelled as a linear heat source with infinite length, i.e. the heat flux is purely radial (Carslaw and Jaeger, 1959 [27]);
- the heat transfer between the borehole and the fluid is governed by the borehole resistance model of Claesson and Eskilson (1988, [28]);

- the minimum (or maximum for cooling mode) temperature reached by the carrier fluid is exactly equal to T_{lim} ;

The G.POT method was derived through the following steps:

- a mathematical method based on the superposition effect was developed in order to calculate the transient temperature alteration at the borehole wall;
- a broad range parametric sweeping was run, under different scenarios, in order to derive the maximum thermal alteration generated over a certain operation time (t_s);
- the results of the above simulations were fitted to derive an empirical relationship with the BHE and site information;
- the derived empirical relationship was then used to estimate the shallow geothermal potential, depending on the depth of the BHE and on the maximum possible thermal alteration of the fluid.

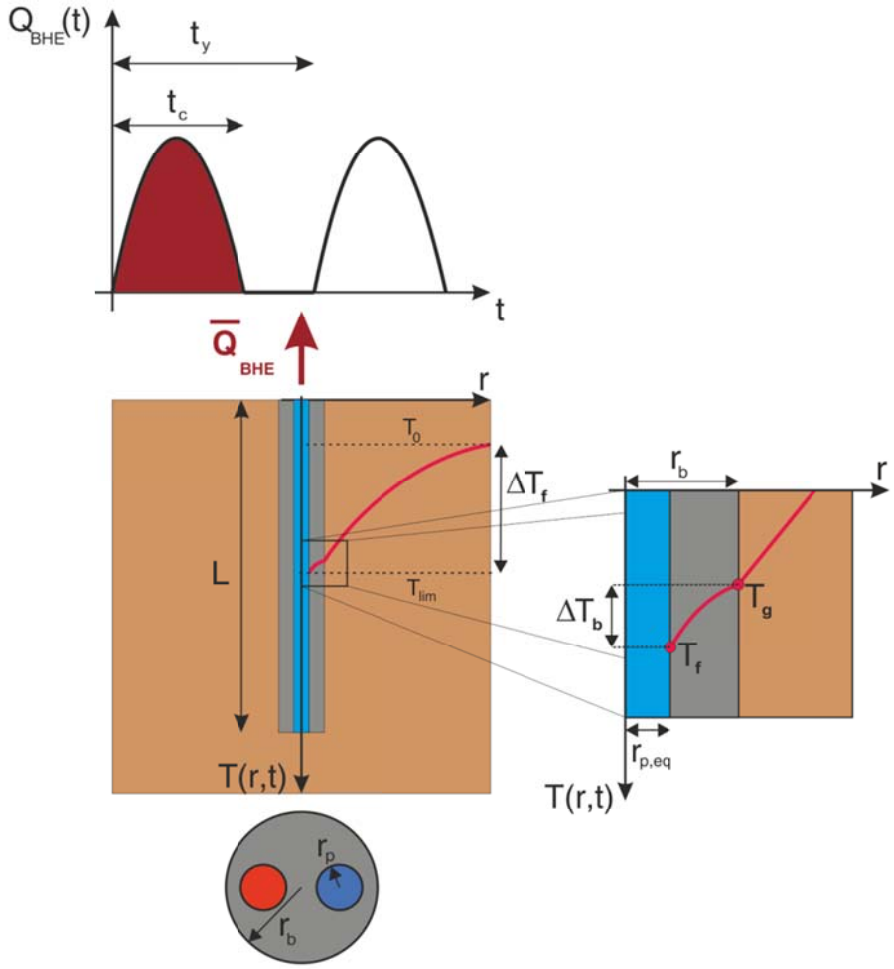

112

113 **Fig. 1 – Input parameters for the estimation of the shallow geothermal potential ($\bar{Q}_{BHE}$) with the G.POT**

114 **method.**

115

116

2.1. Benchmark thermal load function

The benchmark function of the thermal load per unit length $q(t)$ (Wm^{-1}) assumed in the G.POT method has an emi-sinusoidal shape and an annual cycle, as shown in Fig. 1. The cycle is repeated to reproduce the operation of the BHE over its lifetime (t_s). During the annual cycle, heat is exchanged with the ground during a load cycle with a length t_c (i.e., the heating or cooling season), which is followed by a recovery time in which the thermal load is null. The emi-sinusoidal trend was chosen since it reproduces the thermal load of the heating or cooling plant of a building, which is mainly influenced by the external air temperature. The benchmark function $q(t)$ is expressed by the following equation:

$$q(t) = \begin{cases} q_{max} \cdot sin\left(\pi \frac{t}{t_c}\right) & for\ 0 \le t \le t_c \\ 0 & for\ t_c < t \le t_y \end{cases}$$

Eq. 1

where $t_y = 1\ year$. The values of t_c adopted in the simulations range from 30 d to 240 d, and thus cover a wide range of usage profiles, while the average thermal load $\bar{q}$ is equal to 1 $kWhy^{-1}m^{-1}$ (0.114 Wm^{-1}) for all the values of t_c , as shown in Fig. 2. This means that the same heat is exchanged during each year, and hence the results of different simulations are comparable. The amplitude q_{max} depends on the length of the load cycle as shown below:

$$q_{max} = \frac{\pi}{2t_c}\int_0^{t_y} q(t)dt = \frac{\pi}{2t_c} \cdot \bar{q}t_y = \frac{\pi\bar{q}}{2t'_c}$$

Eq. 2

where $t'_c = t_c/t_y$ is the operating time ratio, i.e. the ratio between the lengths of the load cycle and of the year.

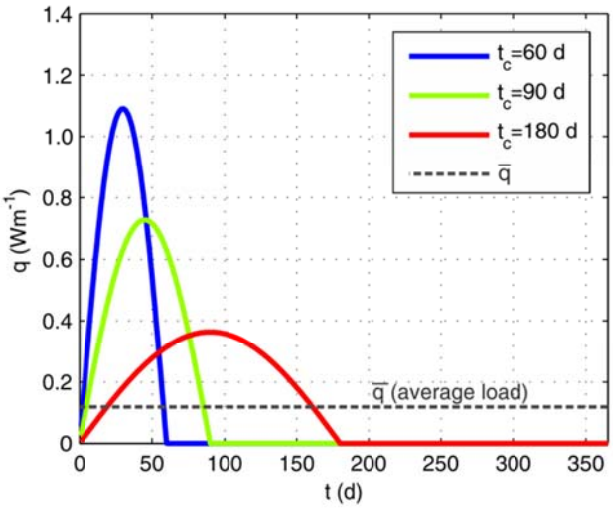

Fig. 2 – Examples of benchmark thermal loads per unit length ($q(t)$) adopted for the simulations with the ILS model, with different load cycle lengths (t_c) and with the same average value ($\bar{q}$).

2.2. Heat transfer in the ground

The thermal load function described in the previous paragraph is the input for a series of heat transfer simulations of a BHE, which were performed with different values of the load cycle length t_c, of the simulated lifetime t_s and of the thermal properties of the ground (λ, ρc). The Infinite Line Source (ILS) model of Carslaw and Jaeger [27] was adopted to calculate the thermal alteration of the ground $\Delta T(r,t)$ that, for a constant thermal load q (Wm^{-1}), is expressed by the following equation:

$$\Delta T(r,t) = \frac{q}{4\pi\lambda} \cdot \int_{r_b^2/(4\alpha t)}^{\infty} \frac{1}{\psi} exp(-\psi) d\psi = \frac{q}{4\pi\lambda} Ei\left(\frac{r^2}{4\alpha t}\right)$$

Eq. 3

where Ei is the exponential integral, and $\alpha = \lambda/(\rho c)$ (m^{2}s^{-1}) is the thermal diffusivity of the ground, i.e. the ratio between the thermal conductivity and the thermal capacity. The ILS model can be adapted for modelling a BHE with a time-varying thermal load, applying the superposition principle to Eq. 3. The thermal alteration of the ground at the borehole wall, i.e. $\Delta T_g(t) = \Delta T(r_b,t)$, is therefore:

$$\Delta T_g(t) = \frac{1}{4\pi\lambda} \cdot \int_0^t \dot{q}(\psi) \cdot Ei\left(\frac{r_b^2}{4\alpha(t-\psi)}\right) d\psi$$

Eq. 4

where $\dot{q}(\psi)$ is the time derivative of the thermal load per unit length q, expressed by Eq. 1.

Eq. 4 was solved numerically with the finite-difference method, approximating the thermal load time series as a piecewise constant function defined over N constant time steps with a length of 1 day. The thermal alteration at the borehole wall is then the superposition of the effects of the single steps q_j, thus:

$$\Delta T_g(t = N \cdot \Delta t) = \frac{1}{4\pi\lambda} \cdot \sum_{j=1}^{N-1} \left[(q_{j+1} - q_j) \cdot Ei\left(\frac{r_b^2}{4\alpha \cdot \Delta t \cdot (N-j)} \right) \right]$$

Eq. 5

An example of a heat transfer simulation with the discretized ILS model of Eq. 5 is reported in Fig. 3. The plot shows that the thermal alteration at the borehole wall progressively decreases during the recovery periods, i.e. when $q(t) = 0$, but the initial temperature is not fully recovered. For this reason, the residual thermal alteration increases over the years and hence the annual maximum thermal alteration has a slow but constantly increasing trend.

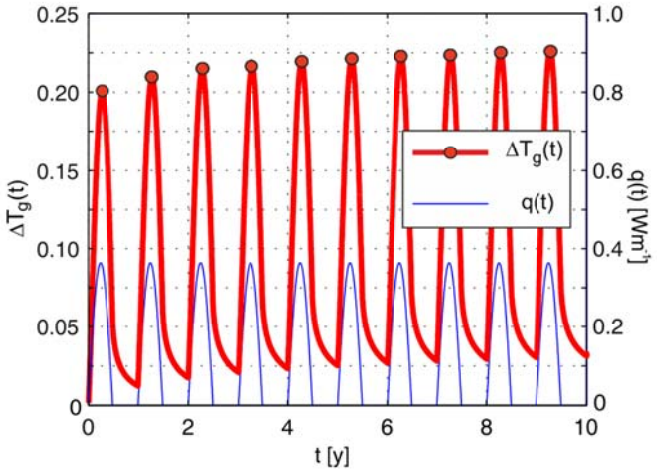

Fig. 3 –Time series of the cyclic thermal load $q(t)$ (thin blue line) and of the thermal alteration at the borehole wall $\Delta T_g(t)$ (thick red line, with red dots on the annual maxima).

2.3. Heat transfer in the borehole (thermal resistance)

The heat transfer inside the BHE was simulated according to the theory of Claesson and Eskilson [28]. Similarly to Ohm's first law, the BHE is also modelled as a thermal resistance R_b between two "nodes", the borehole wall and the "equivalent pipe", i.e. a pipe with the same cross-sectional area of all the pipes of the BHE. The radius of such pipe is $r_{p,eq} = \sqrt{n} \cdot r_p$, where n and r_p (m) are respectively the number and the radius of the pipes (i.e., $n = 2$ for a single U-pipe and $n = 4$ for a double U-pipe). The model considers the average value, thereafter $T_f(t)$, between the inlet and the outlet fluid temperatures. Like a current, the heat flow $q(t)$ induces a temperature difference $\Delta T_b(t)$ (borehole temperature drop) between the borehole wall and the fluid (Fig. 1):

$$\Delta T_b(t) = T_f(t) - T_g(t) = q(t) \cdot R_b$$

Eq. 6

where R_b (mKW^{-1}) is the thermal resistance of the borehole. Eq. 6 describes a local steady-state heat transfer process between the borehole wall and the equivalent pipe. According to [28], such an assumption is valid if the thermal load which varies on a time scale longer than a few hours, for which the effect of the thermal inertia of the borehole can be neglected. This assumption is verified in this work, since the thermal load varies with daily time steps. The value of R_b depends on the geometry of the BHE (number and radius of pipes, distance of pipes), on the physical characteristics of the fluid (flow rate, viscosity, thermal conductivity) and of the borehole filling (thermal conductivity of the geothermal grout). It usually lies in the range $R_b = 0.06 \div 0.12\ mKW^{-1}$ provided by [3], with higher values in single U-pipe boreholes compared to double U-pipes. The borehole thermal resistance can be calculated with a number of methods [29-31]. One of the most commonly adopted was proposed by Shonder and Beck (2000, [32]):

$$R_b = \frac{1}{2\pi\lambda_{bf}} \cdot log\left(\frac{r_b}{r_{p,eq}}\right)$$

Eq. 7

where λ_{bf} (Wm^{-1}K^{-1}) is the thermal conductivity of the borehole filling (geothermal grout) and $r_{p,eq} = \sqrt{n} \cdot r_p$ is the equivalent pipe radius, where n and r_p (m) are respectively the number and the radius of the

188 pipes (i.e., $n = 2$ for a single U-pipe and $n = 4$ for a double U-pipe). A comparison between the modelling
189 approaches of borehole thermal resistance and of the well skin effect [33-35] is reported in the Supporting
190 Information.

191 ### *2.4. Calibration of the simplified heat transfer model*

192 The thermal alteration of the heat carrier fluid $\Delta T_f(t)$ is equal to the sum of the thermal alteration of the
193 ground at the borehole wall $\Delta T_g(t)$ (see Paragraph 2.2) and the borehole temperature drop $\Delta T_b(t)$ (see
194 Paragraph 2.3). The maximum value of $\Delta T_f(t)$ is therefore (Fig. 1):

$$\Delta T_{f,max} = \Delta T_{g,max} + \Delta T_{b,max}$$

195 **Eq. 8**

196 where $\Delta T_{g,max}$ is the maximum thermal alteration at the borehole wall, over the simulation period (i.e., 50
197 years), and $\Delta T_{b,max}$ is the maximum borehole temperature drop.
198 According to Eq. 6, the value of $\Delta T_b(t)$ is directly proportional to the thermal load $q(t)$, and the maximum
199 value is therefore:

$$\Delta T_{b,max} = q_{max} \cdot R_b$$

200 **Eq. 9**

201 In contrast, the maximum value of the thermal alteration at the borehole wall $\Delta T_{g,max}$ cannot be calculated
202 explicitly from Eq. 4. A correlation equation was therefore developed, based on the maximum value of ΔT_g
203 over a certain period, implementing Eq. 5 for different scenarios (see Supporting Information). In analogy
204 to the maximum borehole temperature drop, the value of $\Delta T_{g,max}$ is a function of the maximum thermal
205 load q_{max} according to the following equation:

$$\Delta T_{g,max} = \frac{q_{max}}{4\pi\lambda} \cdot P_{max}$$

206 **Eq. 10**

207 where P_{max} is a non-dimensional function, which was fitted with an empirical relationship reported in Eq.
208 11. The fitting of such relationship was performed over a large number of cases (Tab. 1, for further details
209 refer to the Supporting Information).

$$P_{max}(u'_s, u'_c, t'_c) = p_1 \cdot t'_c \cdot log(u'_s) + (p_2 \cdot t'_c + p_3) \cdot log(u'_c) + p_4 \cdot t'_c + p_5$$

Eq. 11

where $u'_s = r_b^2/(4\alpha t_s)$ depends on the simulation time t_s, $u'_c = r_b^2/(4\alpha t_c)$ depends on the load cycle time t_c, and $t'_c = t_c/t_y$ is the operating time ratio. The calibrated coefficients are $p_1 = -0.619$, $p_2 = 0.532$, $p_3 = -0.962$, $p_4 = -0.455$, $p_5 = -1.619$ The perfect agreement between the simulated data and those provided by the correlation equation (Eq. 11) is shown in Fig. 5.

The maximum thermal alteration of the fluid can therefore be calculated with the following correlation:

$$\Delta T_{f,max} = \frac{q_{max}}{4\pi\lambda} \cdot [-0.619 \cdot t'_c \cdot log(u'_s) + (+0.532 \cdot t'_c - 0.962) \cdot log(u'_c) - 0.455 \cdot t'_c - 1.619 + 4\pi\lambda \cdot R_b]$$

Eq. 12

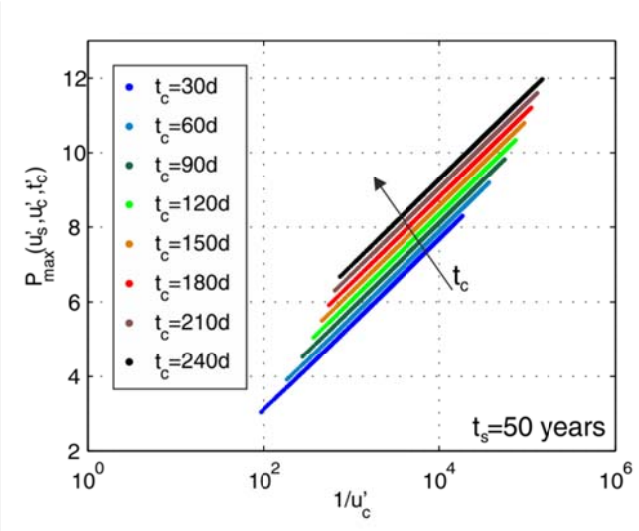

Fig. 4 – Correlation between the reciprocal of the time scale parameter ($1/u'_c = 4\alpha t_c/r_b^2$) and the normalized thermal alteration $P(u'_s, u'_c, t'_c)$, for a simulation time (t_s) of 50 years.

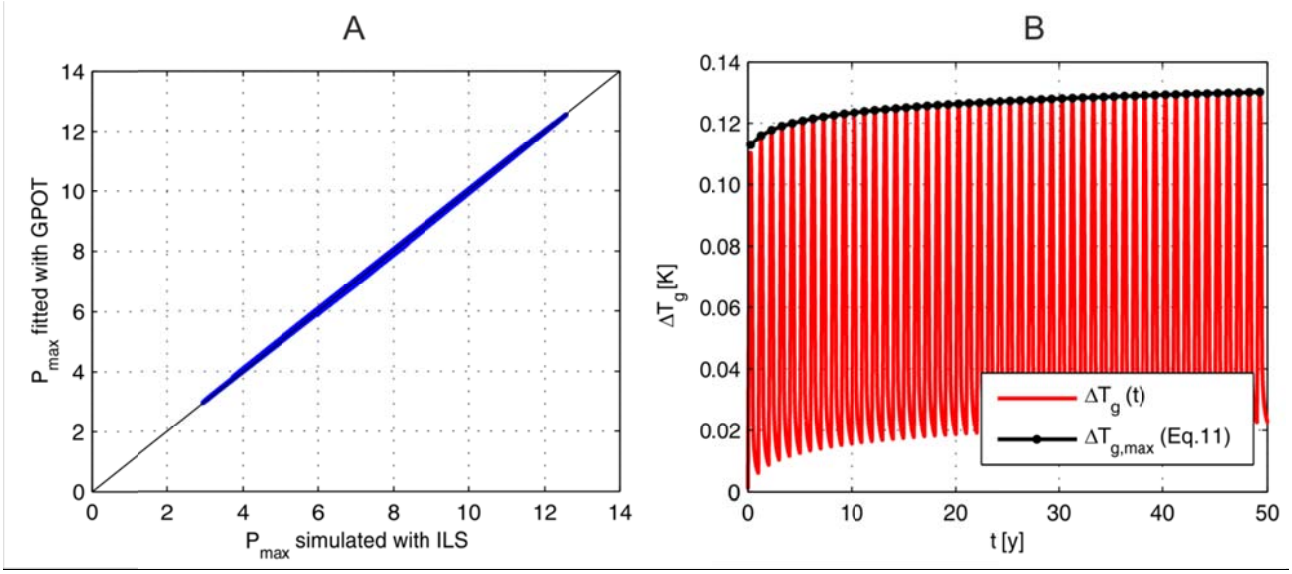

Fig. 5 – Agreement between the results of the heat transfer simulations with the ILS model (Eq. 5) and the fitting with the G.POT method (Eq. 11): A) scatterplot of the non-dimensional function P_{max} calculated with both models; B) comparison of the time trends of $\Delta T_g(t)$ (red line) according to Eq. 5 and of the annual maximum thermal alterations according to Eq. 11 (black line).

Tab. 1 – Values of the parameters adopted in the calibration of Eq. 11.

Parameter	Symbol	Unit	Range of variation	Step
Thermal conductivity of the ground	λ	$Wm^{-1}K^{-1}$	0.2÷1	0.1
			1.2÷10	0.2
Thermal capacity of the ground	ρc	$10^6\ Jm^{-3}K^{-1}$	1÷4	0.2
Length of the heating/cooling season	t_c	d	30÷240	30
Simulation time	t_s	years	10÷100	10
Borehole radius	r_b	m	0.075	-

2.5. Shallow geothermal potential

The value of $\Delta T_{f,max}$ is the specific temperature change of the heat carrier fluid, i.e. the maximum fluid temperature alteration induced by a benchmark thermal load per unit length $q(t)$, with an average value $\bar{q} = 1\ kWh \cdot m^{-1}y^{-1}$. The geothermal potential $\bar{Q}_{BHE}$ is the average thermal load that can be exchanged by a BHE with a length L, inducing a maximum fluid thermal alteration equal to the difference between the

initial temperature T_0 and a threshold value T_{lim}. A proportion can therefore be stated between the average benchmark thermal load ($\bar{q} \cdot L$) and the geothermal potential ($\bar{Q}_{BHE}$):

$$\frac{\bar{q} \cdot L}{\Delta T_{f,max}} = \frac{\bar{Q}_{BHE}}{T_0 - T_{lim}}$$

Eq. 13

Eq. 12 is replaced into Eq. 13 leading to the G.POT relationship to calculate the geothermal potential:

$$\bar{Q}_{BHE} = \frac{a \cdot (T_0 - T_{lim}) \cdot \lambda \cdot L \cdot t_c'}{-0.619 \cdot t_c' \cdot log(u_s') + (0.532 \cdot t_c' - 0.962) \cdot log(u_c') - 0.455 t_c' - 1.619 + 4\pi\lambda \cdot R_b}$$

Eq. 14

where $a = 8$ if $\bar{Q}_{BHE}$ is expressed in W, or $a = 7.01 \cdot 10^{-2}$ is expressed in MWh/y. The geothermal potential is therefore function of the maximum possible thermal alteration of the fluid ($T_0 - T_{lim}$), the thermal conductivity of the ground (λ), the borehole length (L), the thermal resistance of the borehole (R_b) and of three non-dimensional parameters, i.e. $u_s' = r_b^2/(4\alpha t_s)$ depending on the simulation time t_s; $u_c' = r_b^2/(4\alpha t_c)$ and $t_c' = t_c/t_y$ depending the length of the load cycle.

The G.POT method allows for the estimation of the geothermal potential with an explicit correlation, which can be easily implemented in GIS environment or in electronic spreadsheets. An example of the application of the G.POT method is reported in next paragraph.

1. Large-scale mapping of the geothermal potential with the G.POT method

The G.POT method is an easy and flexible tool for the large-scale mapping of the geothermal potential for a single operating mode (only heating or only cooling). If both the operating modes are foreseen, the prevailing one should be considered. This is a conservative assumption, since the balancing effect of the other operating mode is neglected: for example, if the heating mode prevails, the method neglects the fact that the recovery of the ground cooling after the heating season is fostered by the heat injection during the cooling season.

254 Three parameters should be mapped over the surveyed territory, which are the spatial distributions of the
255 undisturbed temperature T_0, the thermal conductivity λ and the thermal capacity ρc of the ground. The
256 length t_c of the heating/cooling season can be the same for the whole area or it can vary over space, e.g.
257 when mapping the geothermal potential in a territory divided into different climate zones, in which the
258 heating/cooling plants are deemed to operate for different time lengths. The other input should be set as
259 uniform, i.e. the operating lifetime t_s, the length L of the BHE, the threshold temperature of the heat
260 carrier fluid T_{lim}, the thermal conductivity λ_{bf} of the grout, the number (n) and the radius of the pipes r_p,
261 and the radius of the borehole r_b.
262 The parameters to be mapped can have a strong spatial variability and the number of data that can be
263 collected is limited. Some examples are therefore shown hereafter on the assumptions that can be made
264 and the empirical relationships that can be adopted to estimate the spatial distributions of the input
265 parameters. These relationships require data which usually have a wide territorial coverage and a good
266 precision, like geological maps, hydrogeological maps and Digital Terrain Models (DTMs).
267 An application of G.POT method is shown in this paper for the mapping of the shallow geothermal potential
268 in the Province of Cuneo, a 6900 km^2 large district in Piemonte, NW Italy. The surveyed territory can be
269 divided into three main areas: the Alpine chain on the southern and western edges, the hills of Langhe and
270 Roero in the north-eastern part of the Province and the large alluvial plain in the central and northern part.
271 The thermal conductivity was mapped adopting two different criteria to assign the values of average
272 thermal conductivity up to a depth of 100 m [36], as reported in the map in Fig. 6:
273 - in the presence of compact rocks like those on the mountains and on the hills, the outcropping
274 lithology resulting from the Geological Map of Piemonte [37] was assigned to the corresponding
275 value of thermal conductivity according to Di Sipio et al. [38]. Such a method was chosen because,
276 for compact rocks, the thermal conductivity mostly depends on the lithology, with a limited
277 influence of the water saturation;

- the alluvial plain is composed of sand and gravel, in which the thermal conductivity is mostly influenced by the water saturation. Two different layers were therefore identified, the vadose zone extending from the ground surface to the water table, where the ground is normally dry, to which a value $\lambda = 0.5\ Wm^{-1}K^{-1}$ was assigned, and the water-saturated layer to which a larger value was assigned ($\lambda = 2.4\ Wm^{-1}K^{-1}$), which is typical of saturated sand or gravel (VDI, 2010 [23]). The assigned value of thermal conductivity is therefore the depth-weighted average of the values of each of these layers.

According to the map in Fig. 6, the highest values of thermal conductivity are observed in the Alpine chain, ranging from 2.5 $Wm^{-1}K^{-1}$ (limestone) to 3.2 $Wm^{-1}K^{-1}$ (granite), with the exception of the clays (1.8 $Wm^{-1}K^{-1}$) outcropping in a belt in the southern part. The hills of Langhe on the right bank of the Tanaro river are mainly composed of marls, with a thermal conductivity of 2.1 $Wm^{-1}K^{-1}$. This value is slightly higher than the one observed in the Roero hills on the left bank of the Tanaro (1.8 $Wm^{-1}K^{-1}$), which are mainly composed of clay and fine sand. In the plain, a rather sharp contrast is observed between the south-western portion, characterized by a high depth to water table and hence a low thermal conductivity (1.2÷1.8 $Wm^{-1}K^{-1}$) and the rest of the plain, in which the water table is shallow and the thermal conductivity is high (2÷2.3 $Wm^{-1}K^{-1}$).

The thermal capacity of the ground was assigned with the same criteria adopted for the thermal conductivity . The interval of variation of the thermal capacity is much narrower compared to the thermal conductivity (1.8÷2.8·10^{-6} $Jm^{-3}K^{-1}$), and its influence on the geothermal potential is therefore much weaker. Further details on the mapping of the thermal capacity of the ground are reported in the Supporting Information.

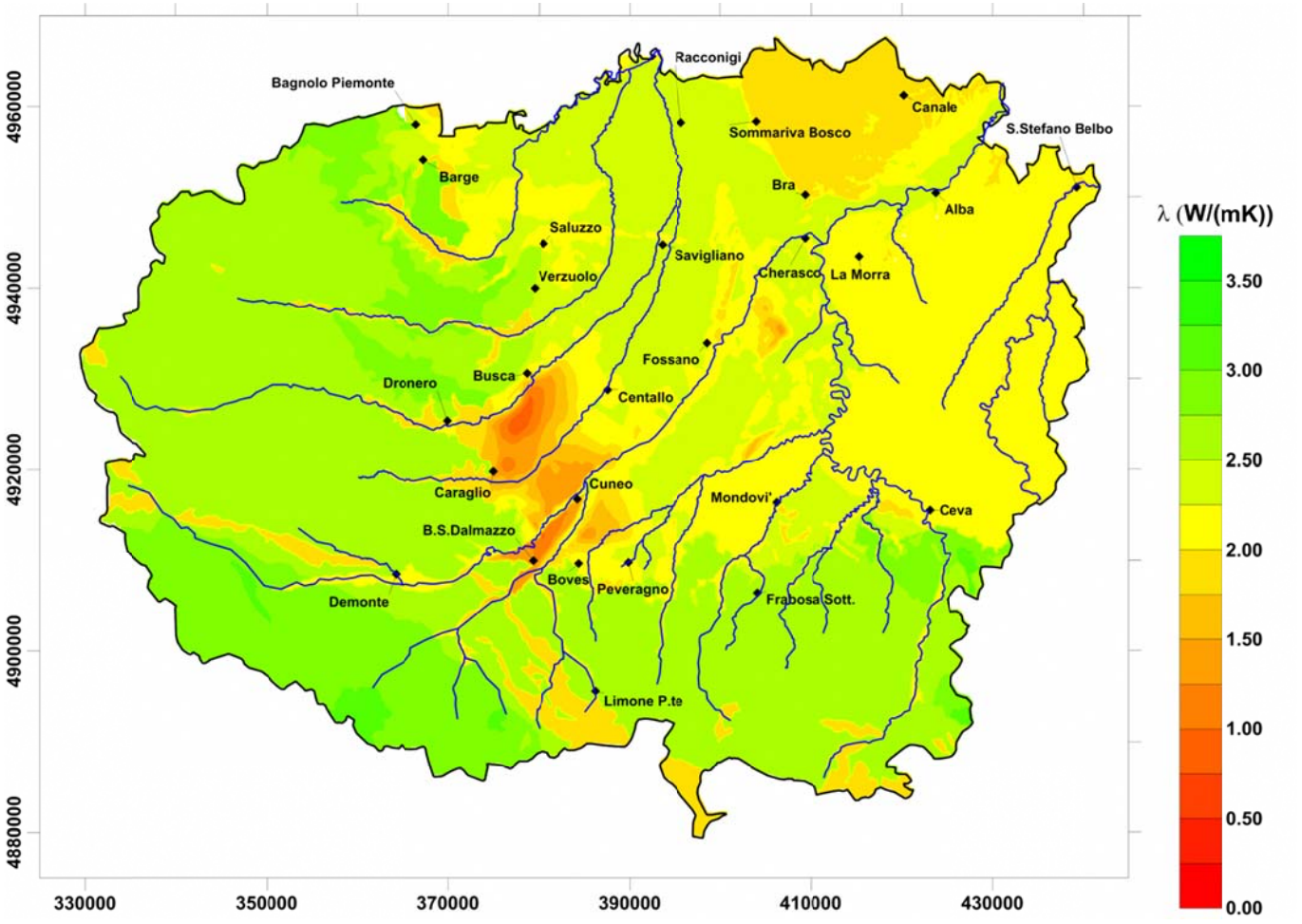

Fig. 6 – Map of the estimated thermal conductivity of the ground λ in the Province of Cuneo, expressed as an average value over 100 m of depth from ground surface.

Data on the undisturbed ground temperature were available only at some water wells on the plain, which are not representative of all the surveyed territory. The empirical formula provided by Signorelli and Kohl [39] was used to estimate the value of T_0:

$$T_0 = 15.23 - 1.08 \cdot 10^{-2} \cdot Z + 5.61 \cdot 10^{-6} \cdot Z^2 - 1.5 \cdot 10^{-9} \cdot Z^3$$

Eq. 15

where Z is the elevation (m a.s.l.), which is available from the Digital Terrain Model (DTM) of Piemonte [40]. The formula reported in Eq. 15 is valid up to an elevation of 1500 m a.s.l., over which the dynamics of the ground temperature are strongly influenced by the snow cover that isolates the ground from the air for

311 a long time during winter. About 25% of the total area is above 1500 m a.s.l. and was therefore excluded by
312 the estimation of the geothermal potential. However, less than 1% of the total population (6000 people)
313 live in this area. In the remaining part of the surveyed territory, the ground surface elevation ranges
314 between 130 and 1500 m a.s.l., and the undisturbed ground temperatures range between 7 and 15°C.
315 The map of the geothermal potential estimated with the G.POT method is reported in Fig. 7. The heating
316 operating mode was considered, with a heating season length of 182 d (e.g., from October 15th to April
317 15th). The calculation were made on a double U-pipe BHE ($n = 4$) with a depth $L = 100\ m$. An operating
318 lifetime (t_s) of 50 years was considered, which is the highest value according to [41]. The radii of the
319 borehole and of the pipes were set respectively to $r_b = 0.075\ m$ and $r_p = 0.016\ m$, and hence the value of
320 the thermal resistance is $R_b = 0.678\ mKW^{-1}$ according to the model of Shonder and Beck (2000, [32])
321 reported in Eq. 7. The threshold temperature of the heat carrier fluid was set to $T_{lim} = -2°C$, which
322 guarantees a good safety margin on the freezing of the heat carrier fluid (e.g., the freezing temperature of
323 a propylene glycol 25% volume concentration is of about -10°C [42]).
324 The geothermal potential map (Fig. 7) indicates that the highest potentiality for thermal extraction (11÷12
325 MWh/y) is in the northern part of the plain (Saluzzo, Racconigi, Savigliano) and along the Tanaro Plain (Bra,
326 Alba, Cherasco), in which both the thermal conductivity and the underground temperature are high
327 (respectively, 2.2÷2.4 $Wm^{-1}K^{-1}$ and 13÷15°C). The hills of Langhe and Roero in the eastern part of the
328 province have a medium potential (8÷10 MWh/y), due to a slightly lower thermal conductivity of the
329 ground (2 $Wm^{-1}K^{-1}$). At the foot of the Alpine chain in the southern and south-western part of the plain
330 between the towns of Busca, Cuneo, Dronero, Caraglio and Borgo San Dalmazzo the ground is
331 characterized by a low thermal conductivity (<1.5 $Wm^{-1}K^{-1}$), due to the presence of a thick unsaturated zone
332 above the shallow aquifer, which can however be exploited for Borehole Thermal Energy Storage (BTES)
333 [43]. In the mountains, very conductive rocks are usually present, but the low ground temperature (<10°C)
334 is a strong limiting factor for shallow geothermal applications for heating purposes.

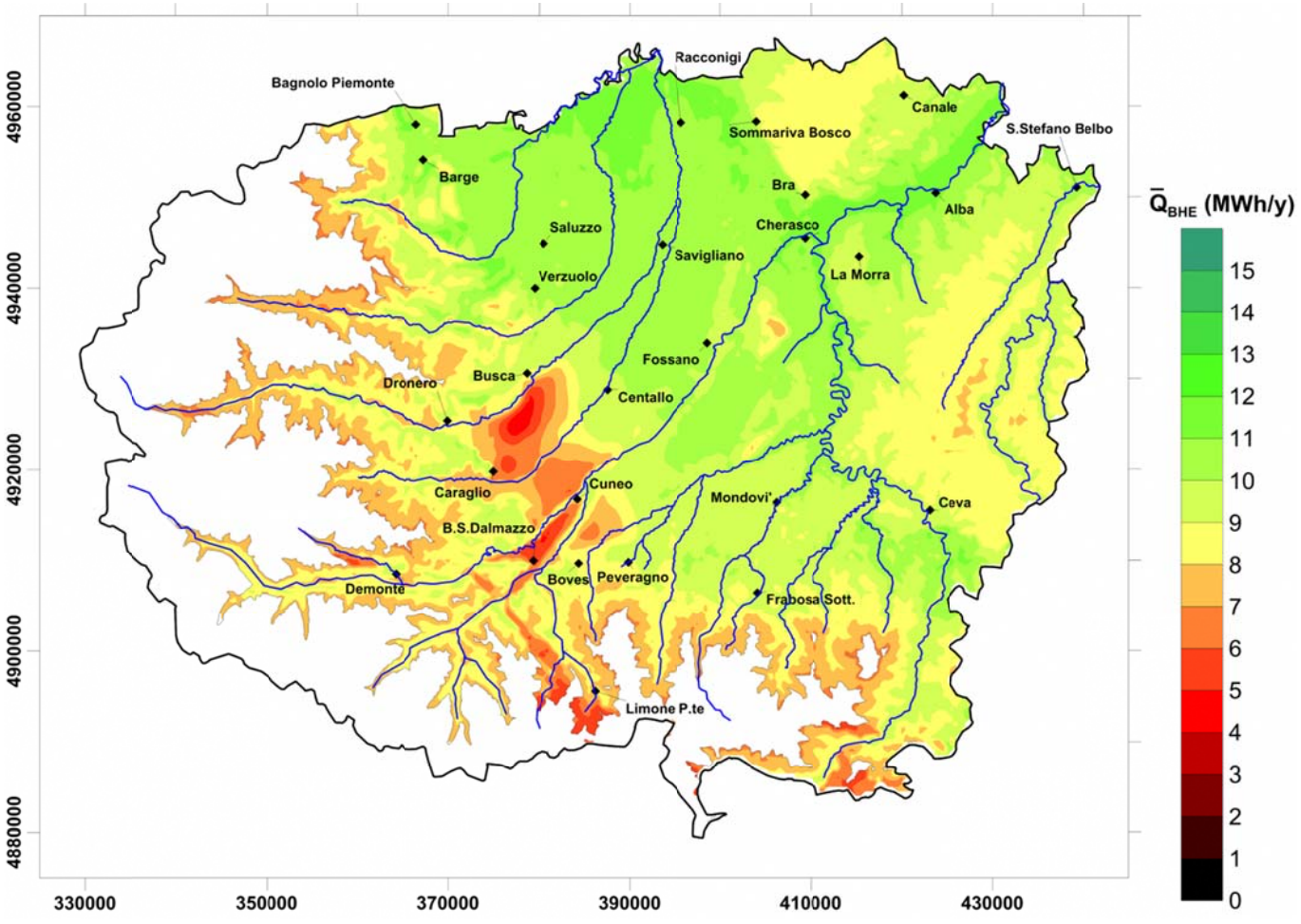

Fig. 7 – Map of the shallow geothermal potential ($\bar{Q}_{BHE}$) of the Province of Cuneo, estimated with the G.POT method for a 100m-long BHE.

2. Conclusions

The shallow geothermal potential, i.e. the thermal power that can be efficiently exchanged by a Borehole Heat Exchanger (BHE) of a certain depth, is an important indicator of the suitability of the ground for the installation of Ground Source Heat Pumps. A method called G.POT was developed to calculate the shallow geothermal potential based on the thermal parameters of the ground (initial ground temperature, thermal conductivity, thermal capacity), of the borehole (thermal resistance) and on the operational and design parameters of the plant (BHE length, threshold temperature of the heat carrier fluid, simulated operation

346 time, duration of the heating/cooling season). The method is based on a simplified heat transfer model of a
347 BHE in a purely conductive medium, which was derived from the results of a large set of heat transfer
348 simulations, adopting a benchmark thermal load profile.
349 The G.POT method was expressively developed for the mapping of the heating or cooling geothermal
350 potential on a large scale. An application was shown in this paper, with the assessment of the heating
351 geothermal potential in the Province of Cuneo, a large district (6900 km^2) in NW Italy. Examples have been
352 shown on how to derive the input data for the G.POT method, based on available geological,
353 hydrogeological and topographic data. The G.POT method proved to be a valuable tool for the mapping of
354 the shallow geothermal potential on a large scale, thus contributing to a wider implementation of this
355 renewable and sustainable heat source.

356 ## Acknowledgements

357 Financial support for this work was provided by Fondazione Cassa di Risparmio di Cuneo in the framework
358 of the project “Survey and mapping of the potentiality of Geothermal Heat Pumps in the Province of
359 Cuneo”.
360

References

[1] Bayer P, Saner D, Bolay S, Rybach L, Blum P. Greenhouse gas emission savings of ground source heat pump systems in Europe: A review. Renewable and Sustainable Energy Reviews. 2012;16(2):1256-67.

[2] Saner D, Juraske R, Kübert M, Blum P, Hellweg S, Bayer P. Is it only CO2 that matters? A life cycle perspective on shallow geothermal systems. Renewable and Sustainable Energy Reviews. 2010;14(7):1798-813.

[3] Florides G, Kalogirou S. Ground heat exchangers—A review of systems, models and applications. Renewable Energy. 2007;32(15):2461-78.

[4] Casasso A, Sethi R. Tecnologia e potenzialità dei sistemi geotermici a bassa entalpia | [Technology and potentiality of geothermal heat pumps]. Geoingegneria Ambientale e Mineraria. 2013;138(1):13-22.

[5] Antics M, Bertani R, Sanner B. Summary of EGC 2013 Country Update Reports on Geothermal Energy in Europe. Conference Summary of EGC 2013 Country Update Reports on Geothermal Energy in Europe, Pisa (Italy). p. 1-18.

[6] Blum P, Campillo G, Kölbel T. Techno-economic and spatial analysis of vertical ground source heat pump systems in Germany. Energy. 2011;36(5):3002-11.

[7] Bristow D, Kennedy CA. Potential of building-scale alternative energy to alleviate risk from the future price of energy. Energy Policy. 2010;38(4):1885-94.

[8] Gemelli A, Mancini A, Longhi S. GIS-based energy-economic model of low temperature geothermal resources: A case study in the Italian Marche region. Renewable Energy. 2011;36(9):2474-83.

[9] Chinese D, Nardin G, Saro O. Multi-criteria analysis for the selection of space heating systems in an industrial building. Energy. 2011;36(1):556-65.

[10] Bertermann D, Klug H, Morper-Busch L, Bialas C. Modelling vSGPs (very shallow geothermal potentials) in selected CSAs (case study areas). Energy. 2014;71(0):226-44.

[11] GEOTRAINET. Annual survey on GSHP market grow - 2010. 2011.

[12] Giambastiani BMS, Tinti F, Mendrinos D, Mastrocicco M. Energy performance strategies for the large scale introduction of geothermal energy in residential and industrial buildings: The GEO.POWER project. Energy Policy. 2014;65(0):315-22.

[13] Karytsas C. Current state of the art of geothermal heat pumps as applied to buildings. Advances in Building Energy Research. 2012;6(1):119-40.

[14] Casasso A, Sethi R. Efficiency of closed loop geothermal heat pumps: A sensitivity analysis. Renewable Energy. 2014;62(0):737-46.

[15] Casasso A, Sethi R. Sensitivity Analysis on the Performance of a Ground Source Heat Pump Equipped with a Double U-pipe Borehole Heat Exchanger. Energy Procedia. 2014;59(0):301-8.

[16] Chung JT, Choi JM. Design and performance study of the ground-coupled heat pump system with an operating parameter. Renewable Energy. 2012;42:118-24.

[17] Angelotti A, Alberti L, La Licata I, Antelmi M. Energy performance and thermal impact of a Borehole Heat Exchanger in a sandy aquifer: Influence of the groundwater velocity. Energy Conversion and Management. 2014;77:700-8.

[18] Dehkordi SE, Schincariol R. Effect of thermal-hydrogeological and borehole heat exchanger properties on performance and impact of vertical closed-loop geothermal heat pump systems. Hydrogeol J. 2014;22(1):189-203.

[19] Molina-Giraldo N, Bayer P, Blum P. Evaluating the influence of thermal dispersion on temperature plumes from geothermal systems using analytical solutions. International Journal of Thermal Sciences. 2011;50(7):1223-31.

[20] Verdoya M, Imitazione G, Chiozzi P, Orsi M, Armadillo E, Pasqua C. Interpretation of Thermal Response Tests in Borehole Heat Exchangers Affected by Advection. World Geothermal Congress 2015. Melbourne, Australia2015. p. 1-7.

[21] Casasso A, Sethi R. Modelling thermal recycling occurring in groundwater heat pumps (GWHPs). Renewable Energy. 2015;77(0):86-93.

[22] Lo Russo S, Taddia G, Verda V. Development of the thermally affected zone (TAZ) around a groundwater heat pump (GWHP) system: A sensitivity analysis. Geothermics. 2012;43:66-74.
[23] VDI. VDI 4640 - Thermal use of underground. Blatt 1: Fundamentals, approvals, environmental aspects2010.
[24] Curtis R, Pine T, Wickins C. Development of new ground loop sizing tools for domestic GSHP installations in the UK. Conference Development of new ground loop sizing tools for domestic GSHP installations in the UK. p. 1-10.
[25] Galgaro A, Di Sipio E, Teza G, Destro E, De Carli M, Chiesa S, et al. Empirical modeling of maps of geo-exchange potential for shallow geothermal energy at regional scale. Geothermics. 2015;57:173-84.
[26] García-Gil A, Vázquez-Suñe E, Alcaraz MM, Juan AS, Sánchez-Navarro JÁ, Montlleó M, et al. GIS-supported mapping of low-temperature geothermal potential taking groundwater flow into account. Renewable Energy. 2015;77(0):268-78.
[27] Carslaw HG, Jaeger JC. Conduction of heat in solids. Cambridge, UK1959.
[28] Claesson J, Eskilson P. Conductive heat extraction to a deep borehole: Thermal analyses and dimensioning rules. Energy. 1988;13(6):509-27.
[29] Bauer D, Heidemann W, Müller-Steinhagen H, Diersch HJG. Thermal resistance and capacity models for borehole heat exchangers. International Journal of Energy Research. 2011;35(4):312-20.
[30] Sharqawy MH, Mokheimer EM, Badr HM. Effective pipe-to-borehole thermal resistance for vertical ground heat exchangers. Geothermics. 2009;38(2):271-7.
[31] Lamarche L, Kajl S, Beauchamp B. A review of methods to evaluate borehole thermal resistances in geothermal heat-pump systems. Geothermics. 2010;39(2):187-200.
[32] Shonder JA, Beck JV. Field test of a new method for determining soil formation thermal conductivity and borehole resistance. Oak Ridge National Lab., TN (US); 2000.
[33] Di Molfetta A, Sethi R. Ingegneria degli Acquiferi: Springer, 2012.
[34] Sethi R. A dual-well step drawdown method for the estimation of linear and non-linear flow parameters and wellbore skin factor in confined aquifer systems. J Hydrol. 2011;400(1–2):187-94.
[35] Van Everdingen A. The skin effect and its influence on the productive capacity of a well. Journal of petroleum technology. 1953;5(06):171-6.
[36] Casasso A, Sethi R. Territorial Analysis for the Implementation of Geothermal Heat Pumps in the Province of Cuneo (NW Italy). Energy Procedia. 2015;78:1159-64.
[37] ARPA Piemonte. Carta della litologia - scala 1:100000. In: ARPA Piemonte, editor.: ARPA Piemonte.
[38] Di Sipio E, Galgaro A, Destro E, Teza G, Chiesa S, Giaretta A, et al. Subsurface thermal conductivity assessment in Calabria (southern Italy): a regional case study. Environmental Earth Sciences. 2014:1-19.
[39] Signorelli S, Kohl T. Regional ground surface temperature mapping from meteorological data. Global and Planetary Change. 2004;40(3–4):267-84.
[40] Regione Piemonte. Modelli digitali del terreno da CTRN 1:10000 (passo 10mt) - Modello altezze filtrato. Open Data Regione Piemonte. Torino: Regione Piemonte; 2000.
[41] Rawlings RHD, Sykulski JR. Ground source heat pumps: A technology review. Build Serv Eng Res Technol. 1999;20(3):119-29.
[42] Dow Chemicals. DOWFROST - Inhibited Propylene Glycol-based Heat Transfer Fluid. Product information. In: Chemicals D, editor.2001.
[43] Giordano N, Comina C, Mandrone G, Cagni A. Borehole thermal energy storage (BTES). First results from the injection phase of a living lab in Torino (NW Italy). Renewable Energy. 2016;86:993-1008.

List of symbols

Acronyms

BHE	Borehole Heat Exchanger
BTES	Borehole Thermal Energy Storage
DTM	Digital Terrain Model
GIS	Geographical Information System
G.POT	Geothermal Potential
GSHP	Ground Source Heat Pump
GWHP	Ground Water Heat Pump
ILS	Infinite Line Source

Latin letters

Symbol	Unit	Description
a	-	Coefficient for the transformation of $\bar{Q}_{BHE}$ in W or MWhy^{-1}
Ei	-	Exponential integral
L	m	Depth of the borehole heat exchanger
N	-	Number of time steps
n	-	Number of pipes
p_1	-	Coefficients of the non-dimensional function P_{max}
p_2	-	
p_3	-	
p_4	-	
p_5	-	
$P_{max}(u'_s, u'_c, t'_c)$	-	Non-dimensional function of the maximum thermal alteration of the ground at the borehole wall
q	Wm^{-1}	Generic constant thermal load per unit length
$q(t)$	Wm^{-1}	Benchmark thermal load per unit length (time-varying function)
$\bar{q}$	Wm^{-1}	Yearly average value of the benchmark thermal load per unit length
$\bar{Q}_{BHE}$	W	Shallow geothermal potential
q_{max}	Wm^{-1}	Maximum value of the benchmark thermal load per unit length
r	m	Generic distance from the Infinite Line Source
r_b	m	Radius of the borehole
r_p	m	Radius of the pipes of the borehole heat exchanger
$r_{p,eq}$	m	Equivalent pipe radius
R_b	mKW^{-1}	Borehole thermal resistance
T_0	K	Undisturbed ground temperature
t	s	Generic time
t_c	s	Length of the load cycle (heating or cooling season)
t'_c	-	Operating time ratio (i.e. the ratio of the length of the load cycle and of the year)
$T_f(t)$	K	Average heat carrier fluid temperature
$T_g(t)$	K	Ground temperature at the borehole wall
$T_{\lim}$	K	Minimum or maximum threshold temperature of the heat carrier fluid

t_s	s	Simulated operation time
t_y	s	Length of the thermal load cycle (i.e. 1 year)
u_c'	-	Non-dimensional cycle time parameter
u_s'	-	Non-dimensional simulation time parameter

462

463 ### *Greek letters*

464

Symbol	Unit	Description
α	m^2s^{-1}	Thermal diffusivity of the ground
Δt	s	Fixed time step length adopted in the calculation of $\Delta T_g(t)$
$\Delta T(r,t)$	K	Thermal alteration at a generic distance r and at a generic time t
$\Delta T_f(t)$	K	Thermal alteration of the heat carrier fluid in response to the benchmark thermal load
$\Delta T_{f,max}$	K	Maximum thermal alteration of the heat carrier fluid in response to the benchmark thermal load per unit length observed in the simulation period t_s
$\Delta T_g(t)$	K	Thermal alteration in the ground at the borehole wall in response to the benchmark thermal load, calculated with the Infinite Line Source model
$\Delta T_{g,max}$	K	Maximum thermal alteration in the ground at the borehole wall in response to the benchmark thermal load, calculated with the Infinite Line Source model
$\Delta T_b(t)$	K	Thermal drop between the borehole wall and the heat carrier fluid
$\Delta T_{b,max}$	K	Maximum thermal drop between the borehole wall and the heat carrier fluid
λ	$Wm^{-1}K^{-1}$	Thermal conductivity of the ground
λ_{bf}	$Wm^{-1}K^{-1}$	Thermal conductivity of the borehole filling (grout)
ψ	-	Dummy integration variable
ρc	$Jm^{-3}K^{-1}$	Thermal capacity of the ground

465

466

467

Figure captions

Fig. 1 – Input parameters for the estimation of the shallow geothermal potential ($\bar{Q}_{BHE}$) with the G.POT method.

Fig. 2 – Examples of benchmark thermal loads per unit length ($q(t)$) adopted for the simulations with the ILS model, with different load cycle lengths (t_c) and with the same average value ($\bar{q}$).

Fig. 3 –Time series of the cyclic thermal load $q(t)$ (thin blue line) and of the thermal alteration at the borehole wall $\Delta T_g(t)$ (thick red line, with red dots on the annual maxima).

REF _Ref442708818 \h * MERGEFORMAT Fig. 4 – Correlation between the reciprocal of the time scale 1*u′c=4atcrb2) and the normalized thermal alteration *Pus′, u′c,tc′, for a simulation time (ts) of 50 years.

Fig. 5 – Agreement between the results of the heat transfer simulations with the ILS model (Eq. 5) and the fitting with the G.POT method (Eq. 11): A) scatterplot of the non-dimensional function P_{max} calculated with both models; B) comparison of the time trends of $\Delta T_g(t)$ (red line) according to Eq. 5 and of the annual maximum thermal alterations according to Eq. 11 (black line).

Fig. 6 – Map of the estimated thermal conductivity of the ground λ in the Province of Cuneo, expressed as an average value over 100 m of depth from ground surface.

Fig. 7 – Map of the shallow geothermal potential ($\bar{Q}_{BHE}$) of the Province of Cuneo, estimated with the G.POT method for a 100m-long BHE.

Tables

Tab. 1 – Values of the parameters adopted in the calibration of Eq.10.

Parameter	Symbol	Unit	Range of variation	Step
Thermal conductivity of the ground	λ	$Wm^{-1}K^{-1}$	0.2÷1	0.1
			1.2÷10	0.2
Thermal capacity of the ground	ρc	$10^6\ Jm^{-3}K^{-1}$	1÷4	0.2
Length of the heating/cooling season	t_c	d	30÷240	30
Simulation time	t_s	y	10÷100	10
Borehole radius	r_b	m	0.075	-